Emergent population dynamics from behavioral optimization in the water column

Emil Friis Frølich, Uffe Høgsbro Thygesen

November 2020

Abstract

Population dynamics in the ocean are generally modelled without taking behavior into account. This in spite of the largest daily feeding times for predators, namely at dawn and dusk, being driven by behavior. The daily pattern stems from the Diel Vertical Migration (DVM). This is usually explained by prey avoiding visual predators, and visual predators seeking to find prey. We develop a game-theoretical model of predator-prey interactions in continuous time and space, finding the Nash equilibrium at every instant. By unifying results for the general resolution of polymatrix games, and a spectral discretization scheme, we can resolve the spatially continuous game nearly instantaneously. Our approach allows a unified model for the slow time-scale of population dynamics, and the fast time-scale of the vertical migration, under seasonal changes. On the behaviorial time-scale, we see the emergence of a deep scattering layer from the game dynamics. On the longer time-scale of population dynamics, the introduction of optimal behavior has a strong stabilizing, compared to the model without optimal behavior. In a changing seasonal environment, we observe a change in daily migration patterns throughout the seasons, driven by changes in both population and light levels. The framework we propose can easily be adapted to population games in inhomogenous terrestrial environments, and more complex food-webs.

1 Introduction

> Jeg synes at fokus skal drejes over på "emergent population dynamics with adaptive behavior" og at DVM "bare" er en illustrerende case".

The diel vertical migration (DVM) is a defining structure of oceanic life, [OHC⁺17]. During the day billions of small fish and zoo-plankton migrate from the upper layers of the ocean to the deeper, darker layers, which can be directly measured as the deep scattering layer, [Sut13, WDI⁺14]. At dusk, the small fish and zoo-plankton migrating upwards, staying in the mixed layer at night to feed. The enornomous vertical movement of copepod and pelagic populations form a vital part of the biological carbon pump, [HV16?].

The mechanisms driving the DVM are not entirely understood, and improving this understanding is a prerequisite for understanding the composition of marine food-webs and mechanisms of carbon transfer. Performing the migration must confer some advantage, measured in terms of increased fitness. A

dominating theory is that the DVM is driven by the attempt of small forage fish copepods shifting to avoid risk from visual predation, and as such is driven by the abundance of light, [NTL$^+$03].

Predators naturally follow their food source, confirmed [SSTM05] with zooplankton feeding baskin sharks following the plankton. The distribution of predators depends on the distribution of prey, and vice versa. In a sense, the predators and prey are playing a game of hide and seek across the water column.

Viewing the DVM as an emergent phenomenom from behavorial optimization was pioneered by [Iwa82]. Qualitive characteristics of the DVM emerged purely from behavior, such as the emergence of the deep scattering layer, and a mixing of predators and prey in the mixed layer at night. This was accomplished by discretizing the water column in two zones, an upper layer and a dark lower layer. The day-night cycle into a day and night stage, neglecting dawn and dusk. Neglecting dawn and dusk is a critical oversight as the migration acts a driver of ocean population dynamics, with a majority of predator-prey interactions taking place at dusk and dawn in the mixed layer, [BBM14].

Advances in computational power and new modelling approaches have led to an exploration of models with continuous space and discontinuous time, [PV19], and models with continuous space and time [TP18]. Expanding the complexity of the models allows prediction of fine-grained dynamics of the vertical migration, such as the exact location and size of the deep scattering layer, and the magnitude of feeding at dawn and dusk.

Models of poulation dynamics generally do not incorporate optimal behavior, with notable exceptions, [? ?]. In particular, in previous models with a continuous spatial dimension, modeling population dynamics has been infeasible, [?].

In this paper we present a new modelling approach for population games in continuous space, applied to the diel vertical migration. Our model is a modification of the model studied in [TP18]. We rephrase the vertical game as a linear complementarity problem, [MZ91], which can solved efficiently. Our approach provides a unified framework for examining the population and behavorial time-scales. Unifying the two time-scales allows us to examine how the vertical distribution of predators and prey change throughout the seasons and how this influences the population dynamics. We investigate the length and magnitude of the feeding rates of predators and consumers at dusk and dawn in spring, summer and autumn. In this way we model a the population dynamics associated to a single spawning cycle, and do not need to take ontogenics into account.

Organisms in game-theoretical models are usually seen as perfectly rational, acting on perfect state information. This seems patently unreasonable, as fish and zooplankton do not have perfect information on the state of the water column. In addition the minor gain in fitness from the almost-perfect choice to the perfect choice seems like it would be outweighed by the higher cognitive or sensorial cost of finding the perfect strategy. We incorporate this feature in our model by letting the animals maximize an expectation value with respect to their strategy, and letting their strategy incorporates noise. This allows us to examine how the optimal behavior with noise differs from that without noise, and how it changes the population dynamics. Again, this is feasible due to the numerical scheme we have chosen to examine the system. A change away from full rationality is expected to impact the fitness negatively, but it is unclear by
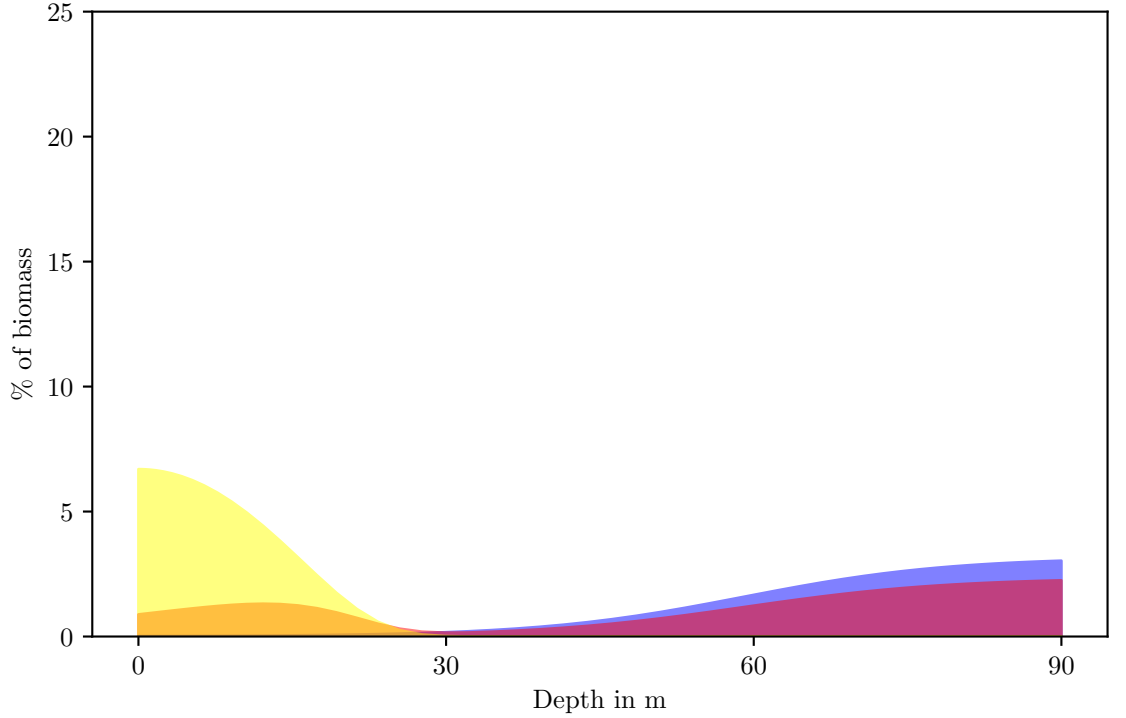
2

Figure 1: Sketch of model ecosystem, showing example distribution of resources, $(r(z,t)/R(t)$ *(yellow)*, consumers ,φ_c *(blue)* and predators, φ_p *(red)*

how much. We examine this by looking at the population dynamics for the fully rational organisms compared to those with bounded rationality. As a baseline, we compare against the system with no behavorial optimization to see how the population dynamics evolve.

2 Model

Model introduction

We consider a food-chain in a water column, consisting of a resource R with concentration, a consumer C, and a predator P. The resource is thought of as phytoplankton, the consumer as copepods and the predator as forage fish. The predators and consumers are each distributed in the water column according to probability distributions, φ_c, φ_p, and the resource is distributed according to $r(z,t)$. See Section 2

Forage fish are visual predators, so their predation success is heavily light dependent. The available light decreases with depth in the water column, and varies with the time of day. The light intensity I at depth z is approximately $I(z) = I_0 \exp(-kz)$, and the light-dependent clearance rate of a predator is $\beta_{p,0}$. However, even when there is no light available there is still a chance of catching

3

a consumer if it is directly encountered, so the clearance rate, $\beta_p(z,t)$, of forage fish never goes to 0 even at the middle of the night or at the deepest depths.

$$\beta_p(z,t) = \beta_{p,0} \frac{I(z,t)}{1 + I(z,t)} + \beta_{p,min}$$

We model the light-levels at the surface via. the python package pvlib, using a simple Clear Sky model in Oresund between Denmark and Sweden. The light levels are given by the direct horizontal light intensity at the sea-surface, neglecting more complicated optic effects. The model takes the precitibale water w_a, and aerosol optical depth, *aod*. We model light decay throughout the water column as $\exp(-kz)$.

In contrast to forage fish, copepods are olfactory predators, and their clearance rate, β_c, is essentially independent of depth and light levels.

$$\beta_c(z,t) = \beta_{c,0}$$

The interactions between the consumer and resource are local, as are the interactions between a predator and a consumer. The local encounter rate between consumers and resources is given by $\beta_c(z,t)c(z,t)r(z,t)$, and the local encounter rate between predators and consumers is $\beta_p(z,t)c(z,t)p(z,t)$.

Population dynamics

The resource cannot move actively, so its time dynamics are naturally specified locally. The growth of the resource is modeled with a logistic growth, with a loss from grazing by consumers and diffusion from the natural movement of the water. To simplify the model, we assume interactions can be described with a Type I functional response.

The total population growth of the consumer population is found by integrating the local grazing rate over the entire water column multiplied by a conversion efficiency ε, subtracting the loss from predation. The growth of the predators is given by the predation rate integrated over the water column:

$$\dot{r} = r(z,t)\left(1 - \frac{r(z,t)}{r_{max}(z)}\right) - \beta_c(z,t)\varphi_c(z,t)C(t)r(z,t) + k\partial_z^2 r(z,t) \tag{1}$$

$$\dot{C} = C(t)\left(\int_0^{z_0} \varepsilon\beta_c(z,t)\varphi_c(z,t)r(z,t)dz - P(t)\int_0^{z_0}\beta_p(z,t)\varphi_c(z,t)\varphi_p(z,t)dz - \mu_C\right) \tag{2}$$

$$\dot{P} = P(t)\left(C(t)\int_0^{z_0}\varepsilon\beta_p(z,t)\varphi_c(z,t)\varphi_p(z,t)dz - \mu_P\right) \tag{3}$$

Fitness proxies and optimal strategies

The instantaneous fitness pr. capita of a forage fish (F_p) or copepod (F_c) is given by the total growth divided by the biomass. We arrive at the fitness by dividing the population growth rate Equation (3) by the total populations, eliminating the terms $C(t), P(t)$ outside the parantheses in Equation (3).

$$F_c(\varphi_c, \varphi_p) = \int_0^{z_0} \varepsilon \beta_c(z,t) \varphi_c(z,t) r(z,t) dz \tag{4}$$

$$- P(t) \int_0^{z_0} \beta_p(z,t) \varphi_c(z,t) \varphi_p(z,t) dz \tag{5}$$

$$F_p(\varphi_c, \varphi_p) = C(t) \int_0^{z_0} \varepsilon \beta_p(z,t) \varphi_c(z,t) \varphi_p(z,t) dz \tag{6}$$

At any instant, an organism seeks to find the strategy that maximizes its fitness. A strategy in our case is a probability distribution in the water column. The optimal strategy φ_c^* of a consumer depends on the strategy of the predators, and likewise for φ_p^* for the predators. Denoting the space of probability distributions on $[0, z_0]$ by $\mathbb{P}(0, z_0)$, this can be expressed as:

$$\varphi_c^*(z,t)(\varphi_p) = \mathrm{argmax}_{\varphi_c \in \mathbb{P}(0,z_0)} \int_0^{z_0} \varepsilon \beta_c(z,t) \varphi_c(z,t) r(z,t) dz$$

$$- P(t) \int_0^{z_0} \beta_p(z,t) \varphi_c(z,t) \varphi_p(z,t) dz$$

$$\varphi_p^*(z,t)(\varphi_c) = \mathrm{argmax}_{\varphi_p \in \mathbb{P}(0,z_0)} C(t) \int_0^{z_0} \varepsilon \beta_p(z,t) \varphi_c(z,t) \varphi_p(z,t) dz$$

Consumers and predators maximize their fitness simultaneously, leading to a *Nash Equilibrium*, where neither can gain anythin from diverging from their strategy. The Nash equilibrium of the instantaneous game is:

$$\varphi_c^{*,NE} = \mathrm{argmax}_{\varphi_c \in P(0,z_0)} \int_0^{z_0} \varepsilon \beta_c(z,t) \varphi_c(z,t) r(z,t) dz \tag{7}$$

$$- P(t) \int_0^{z_0} \beta_p(z,t) \varphi_c(z,t) \varphi_p^{*,NE}(z,t) dz \tag{8}$$

$$\varphi_p^{*,NE} = \mathrm{argmax}_{\varphi_p \in P(0,z_0)} C(t) \int_0^{z_0} \varepsilon \beta_p(z,t) \varphi_c^{*,NE} \varphi_p(z,t) dz \tag{9}$$

Noisy strategies

Our model incorporates that fish are not necessarily perfectly rational, but have **bounded rationality** by letting the strategy depend on the rationality parameter σ, with $\sigma = 0$ being completely rational and $\sigma = \infty$ completely irrational. Rather than choosing a precise location, an individual can choose where it diffuses around. As fish cannot swim out of the top of the ocean, nor through the bottom, we end with the partial differential equation:

$$\partial_\sigma \varphi_i = \partial_z^2 \varphi_i \tag{10}$$

$$\partial_z \varphi_i \mid_{z=0} = 0 \tag{11}$$

$$\partial_z \varphi_i \mid_{z=z_0} = 0 \tag{12}$$

The equation Equation (10) has the fundamental solution $f_Y(\sigma)$, determined by the method of images. Instead of choosing a distribution φ, an individual chooses a distribution f_X, which we use as initial condition in Equation (10). An individual with strategy f_X will actually be distributed according to $\varphi(\sigma, z)$,

which becomes increasingly uniform as σ increases. The way we concretely solve ?? with initial condition f_X is through a Greens function approach, ie. performing a convolution of f_X and f_Y. We refer to the solution φ of Equation (10) as the realized distribution.

We expect that an individual will still attempt to maximize its own fitness, even though the location cannot be chosen exactly. Instead, the optimization will go towards finding the strategy f_X that maximizes the fitness when noise is taken into account. Having introduced noise to the strategies of consumers and predators, we can find the Nash equilibrium of their optimal distributions without noise. We find the Nash pair by inserting the fundamental solution in Equation (7) and optimizing over f_{X_i}, $i \in \{c, p\}$.

$$f_{X_c}^{*,NE} = \mathrm{argmax}_{f_{X_c} \in \mathbb{P}(0, z_0)} \int_0^{z_0} \varepsilon \beta_c(z, t)(f_{X_c} * f_Y)r(z, t)dz$$
$$- P(t) \int_0^{z_0} \beta_p(z, t)(f_{X_c} * f_Y)(f_{X_p}^{*,NE} * f_Y)dz$$
$$f_{X_p}^{*,NE} = \mathrm{argmax}_{f_{X_p} \in \mathbb{P}(0, z_0)} C(t) \int_0^{z_0} \varepsilon \beta_p(z, t)(f_{X_c}^{*,NE} * f_Y)(f_{X_p} * f_Y)dz$$

The realized distributions are found by convolution with f_Y as

$$\varphi_c^{*,NE} = f_{X_c}^{*,NE} * f_Y$$
$$\varphi_p^{*,NE} = f_{X_p}^{*,NE} * f_Y$$

Spatial discretization

We discretize the interval $[0, z_0]$ with a spectral scheme based on Legendre polynomials, [Kop09], which allows precise integration and differentation with only relatively few points. We approximate pure strategy of being in a point z_i by a normalized hat-function e_i, zero everywhere apart from z_i.

$$\int_{z_i}^{z_{i+1}} e_i dz = 1$$
$$e_i(z_{i-1}) = 0, \ e_i(z_{i+1}) = 0$$

Working on a grid with N points, a strategy chosen by a consumer or predator then becomes a linear combination of hat-functions,

$$\varphi_i = \sum_{j<N} a_{j,i} e_j, \quad i \in \{c, p\}$$
$$\sum_{j<N} a_{j,i} = 1 \quad i \in \{c, p\} todo$$

The strategy of a player is fully determined by the a_i's.

When considering non-optimal actors, we need to implement the convolution with f_Y, which also assures that the resulting distrbution is smooth. An added benefit of incorporating bounded rationality then becomes that our strategy profiles are guaranteed to be smooth, decreasing the number of points needed for exact evaluation of the integrals.

Finding the Nash Equilibrium and time-stepping

Finding the Nash Equilibrium in a game in continuous space is usually a very hard task, requiring the development of bespoke methods, [TP18], or very long runtimes, [PV19]. The method we have use circumvents these problems, by combining a little-known result in mathematical optimization with a spectral scheme.

By discretizing space, we have reduced an uncountable strategy set to a more manageable finite amount, with pure strategies e_i. The gain of a consumer playing strategy e_i against a predator playing strategy e_j can be determined as $F_c(e_i, e_j)$, Equation (6), and similarly for a predator. Both payoff functions are bi-linear in the strategies, which allows us to write up payoff matrices E_c, E_p, with entry (i, j) determined through $F_k(e_i, e_j), k \in \{c, p\}$. If a predator plays strategy s_p, given by a vector $(a_1, \ldots, a_N)$ and a consumer plays strategy s_c given by $(b_1, \ldots, b_N)$, the consumer and predator payoffs can be determined through E_c, E_p as:

$$F_c(s_c, s_p) = \langle s_c, E_c s_p \rangle$$
$$F_p(s_c, s_p) = \langle s_p, E_p s_c \rangle$$

Our discretization has reduced the problem to a bimatrix game, where finding the Nash equilibrium is more tractable.

> Jeg synes vi skal fjerne den efterfølgende sætning, da den ikke bidrager til klarhed. Polymatrixspil kan evt. nævnes som en mulig generalisering i diskussionen: A bimatrix game is a special case of a polymatrix game, where n players play against each other in pairwise games and the total payoff is given by the sum of the payoffs across the pairwise interactions.

It does not appear to have diffused through the literature, but a Nash equilibrium of a bimatrix game can be found by solving a linear complementarity problem [MZ91]. We repeat the argument from [MZ91], specialized to the case of two-player games: Assume that (s_c, s_p) constitute a Nash equilibrium in mixed strategies with values $\gamma_c = \langle s_c, E_c s_p \rangle$ and $\gamma_p = \langle s_p, E_p s_c \rangle$ to the consumer and predator, respectively. Then

> Jeg har vist indført lidt inkonsistent notationen her ...

$$\langle s_p, e_p \rangle = \langle s_c, e_c \rangle = 1$$

since these mixed strategies are probability distributions on strategy space. Here e_c and e_p are the "one" functions. In addition the Nash equilibrium dictates

> Or vectors? Clarify setting.

$$E_c s_p = \gamma_c e_c - w_c, \quad E_p s_c = \gamma_p e_p - w_p$$

w_c and w_p are non-negative "slack variables" that state that the payoff for the e.g. the consumer can be no greater than the expected payoff γ_c, but can be smaller for some fixed strategees. These non-optimal strategies, where the slack w_c is positive, must then be chosen with probability 0, and as a consequence the complementarity condition

$$\langle s_c, w_c \rangle = \langle s_p, w_p \rangle = 0$$

holds. Assume for convenience that all elements in E_c and E_p are negative; this can always be obtained without changing the Nash equilibria by substracting a

constant from E_c and E_p. Consequenty, also the payoffs γ_c and γ_p are negative and thus the vector $z = (s_c, s_p, -\gamma_c, -\gamma_p)$ satisfies the Linear Complementarity Problem (LCP)

$$z \geq 0, w \geq 0, Hz + \begin{pmatrix} 0 \\ 0 \\ -1 \\ -1 \end{pmatrix} = w, \quad \langle z, w \rangle = 0.$$

where

$$H = \begin{bmatrix} 0 & -E_c & -e_c & 0 \\ -E_p & 0 & 0 & -e_p \\ e_c & 0 & 0 & 0 \\ 0 & e_p & 0 & 0 \end{bmatrix}$$

Conversely, assume that $z = (s_c, s_p, \gamma_c, \gamma_p)$ and w solve the Linear Complementarity Problem, then it is straightforward to see that the mixed strategies (s_c, s_p) form a Nash equilibrium with values (γ_c, γ_p). The assumption that E_c and E_p have negative elements imply that the matrix H is copositive plus (meaning, for all $z \geq 0$ with $z \neq 0$ it holds that $\langle z, Hz \rangle > 0$) which is a requirement for some algorithms for solving LCP's, in particular Lemke's algorithm.

Therefore our approach provides an avenue to reduce the intractable problem of finding a Nash equilibrium of a multiplayer game in continuous space to solving an optimization problem. When solving the linear complementarity problem, the first step is to introduce the total payoff matrix:

$$R_{init} = \begin{bmatrix} 0 & E_c \\ E_p & 0 \end{bmatrix}$$

As all entries in R_{init} do not have the same sign, R_{init} is not copositive. We fix this by defining $R = R_{init} - max(R_{init})$. Applying the results of [MZ91], to find the Nash equilibrium we need to solve the problem:

$$(Hz + q) = w \tag{13}$$
$$\langle z, w \rangle = 0 \tag{14}$$
$$z \geq 0, w \geq 0 \tag{15}$$

where

$$H = \begin{bmatrix} -R & -A^T \\ A & 0 \end{bmatrix}$$
$$A = \begin{bmatrix} -1 & \dots & -1 & 0 & \dots & 0 \\ 0 & \dots & 0 & -1 & \dots & -1 \end{bmatrix}$$
$$q = \begin{pmatrix} 0 & \dots & 0 & -1 & \dots & -1 \end{pmatrix}$$

Solving Equation (15) was done through two different methods. The interior-point method as implemented in IPOPT, [WB06], called via. the auto-differentation software CasADi [AGH$^+$19], and Lemkes Algorithm implemented in the Numerics package in Siconos, [ABB$^+$19]. Experience showed that Lemkes algorithm was the fastest, but there is probably a situation where the problem has a sparsity structure favorable to IPOPT.

With a fast algorithm for finding the Nash Equilibrium in hand, we are able to solve the time-dynamics for the predator-prey system by a Euler-scheme. The dynamics of the resource are more complicated due to the diffusion term, Equation (3). We solve the partial differential equation for the resource using the method of exponential time-differencing with a first-order approximation of the integral. Using exponential time-differencing guarantees a stable solution, though the system may be stiff, [HO10].

Model parametrization

Following [?], we parametrize the clearance and loss rates in a metabolically scaled manner following Kleibers law, [?], using scaling constants from [And19]. We use the default parameters in the clear-sky model, modelling a sequence of moonless nights. This is a bit of a simplification, but it should not have a great effect on our results. The North Sea is modeled with a rather high attenueation coefficient.

|		
Precipitable water	w_a	$1 \text{ g} \cdot \text{m}^{-3}$
Aeorosol optical depth	aod	0.1
Light decay	k	0.1 m^{-1}
Ocean depth	z_0	90 m
Consumer mass	m_c	$0.05 \text{ } g$
Predator mass	m_p	$20 \text{ } g$
Consumer clearance rate	β_c	$32 \text{ m}^3 \text{ year}^{-1}$
Predator clearance rate	β_p	$2800 \text{ m}^3 \text{ year}^{-1}$
Consumer metabolic rate	μ_c	$0.24 \text{ g}^3 \text{ year}^{-1}$
Predator metabolic rate	μ_p	$21 \text{ g}^3 \text{ year}^{-1}$
Minimal attack rate	β_0	$5 \cdot 10^{-3} \beta_p$
Phytoplankton growth	λ	100 year^{-1}
Phytoplankton max	r_{max}	$10\mathcal{N}(0,6) \text{ g·m}^{-1}$
Irrationality	σ	$14 \text{ } m^2$
Diffusion rate	k	$500 \text{ m}^2 \text{ year}^{-1}$

3 Results
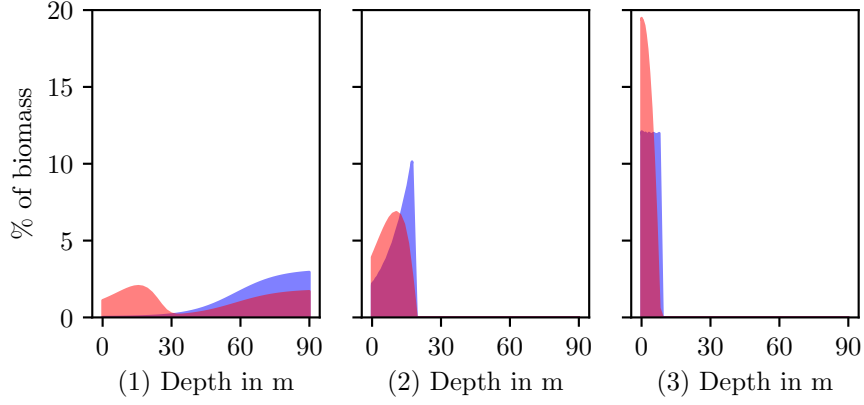
Figure 2: Daily distribution of consumers *blue* and predators *red* at noon *(1)*, dusk *(2)* and at midnight, *(3)* with full rationality on the 1st of October

At noon, Figure 2(1) the consumers form a deep scattering layer, where most of the predators are also present, excepting a few hanging out higher in the water column deterring upward consumer migration Figure 2(1)(15 m), corresponding to the modelling results of [PV19].

At dusk, Figure 2(2) the predators have a greater concentration near the surface, while the consumer "box" is begining to form, yet still with a continuous drop-off to the surface due to the risk from the light. At midnight Figure 2(3) the consumers are concentrated near the surface, with a discontinuous drop to nothing. The predators follow the consumers, albeit with a continuous shape, both distributions being similar to the results of [TP18].
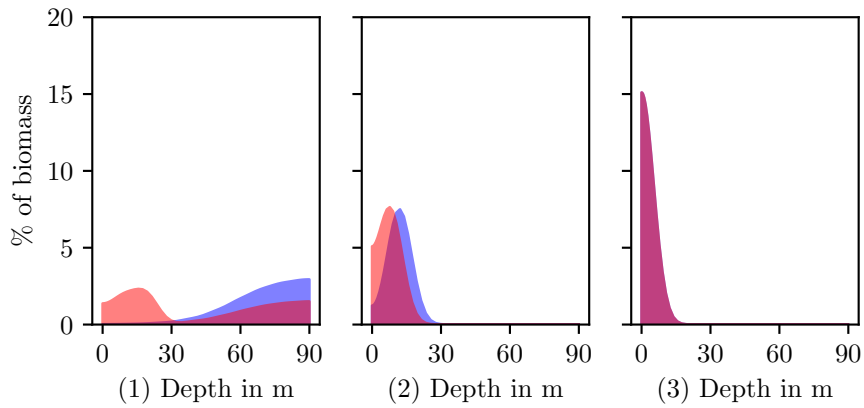

Figure 3: Daily distribution of consumers *blue* and predators *red* at midnight *(1)*, noon *(2)* and at 18:45, *(3)* with bounded rationality

Examining snapshots of the migration in the ecosystem with bounded rationalty, **??**, we see roughly the same picture as in Figure 2. The greatest difference is at midnight and dusk, **??**(1,3), where the bounded rationality leads to a smooth shape for the distrbution of consumers. At noon, the distributions in the system with bounded rationality **??**(2) and Figure 2(2) are almost entirely equal. The shapes of the distributions at both day and night seem to agree better with observations in the model with bounded rationality, [VSSK01, HKM91], lending credence to the idea that copepods are not perfectly rational.
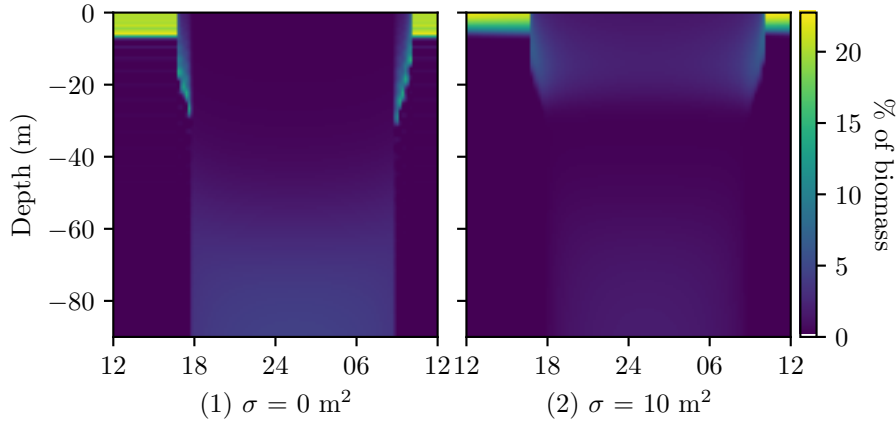

Figure 4: Vertical distribution of consumers *(1)* and predators *(2)* throughout the 1st of July. The time is in hours from noon.

To understand the migration in greater detail, we look at the complete migration picture. The vertical migration of consumers, Figure 4(1) is clear here in the middle of the summer.They are highly concentrated at the top of the water column during nighttime, and at day they scatter throughout the deep. The pattern of the predators is slightly different from the consumer pattern, Figure 4. At nighttime there is still a non-zero concentration of predators in the upper layers of the water-column, there to catch any errant prey.
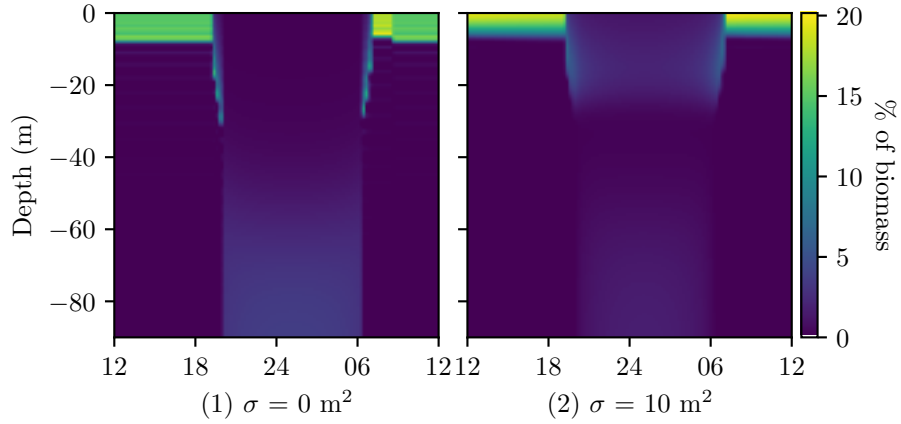
Figure 5: Vertical distribution of consumers *(1)* and predators *(2)* throughout the 1st of October. The time is in hours from noon.

Moving the hands on the clock forward to October, we again see a clearly defined vertical migration, Figure 5. The migration differs from the previous migration, in that the descent and ascent are steeper, and the distributions are wider during the night. That vertical migrations change seasonally due to changes in nutrient and light has been studied in the arabian sea, [WDI+14], and our method enables testable predictions of how this seasonal migration can vary, allowing comparison with large empirical studies [?].
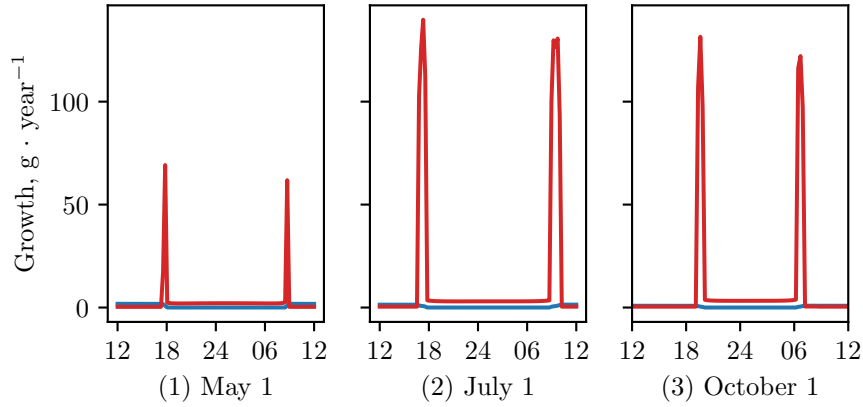

Figure 6: Seasonal comparison of consumer *(blue)* and predator, *(red)* feeding patterns on 1st of May *(1)*, 1st of July *(2)* and 1st of October *(3)*

At all three points in time, consumers have a constant feeding level throughout the night Figure 6. The main feeding time for predators is at dawn and dusk, with a slight peak during the day as well, Figure 6. The length of predator feeding duration increases with the length of the night, Figure 6(2,3). Peak predator feeding activity decreases by a factor of 3/4 throughout the seasons,
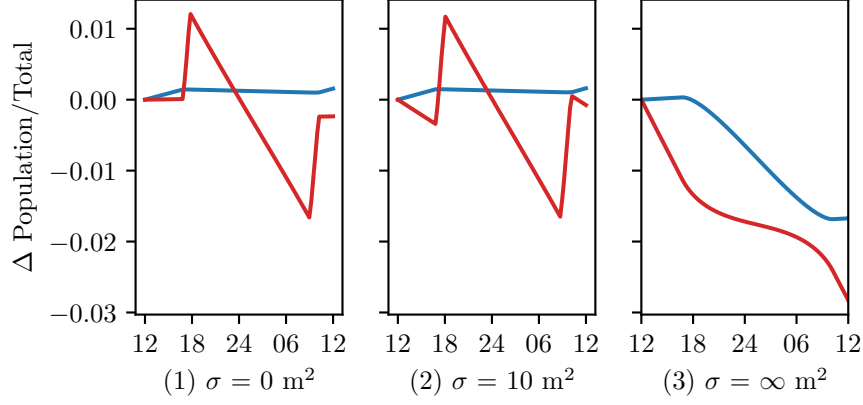
Figure 6, reflecting lower maximal light levels.

Figure 7: Comparison of consumer *(blue)* and predator, *(red)* pr. capita growth patterns with complete rationality *(1)*, bounded rationality *(2)* and full irrationality *(3)*

Looking at short-term population growth in the model with full rationality and bounded rationality, Figure 7(1,2), the change in consumer and predator populations throughout a day is on the order of 10^{-3}. In contrast, the model with constant behavior has rather large fluctuations of populations through a single day Figure 7(3).
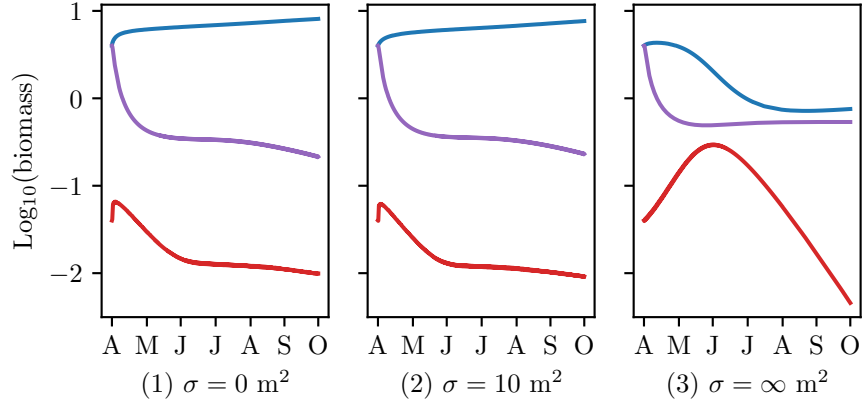

Figure 8: Total populations of consumers *(blue)*, predators, *(red)* and resources *(purple)* from 1st of april to 1st of october. We vary the rationality, from total rationality *(1)*, bounded rationality ($\sigma = 10$), *(2)* and fully irrational, $\sigma = \infty$, *(3)*.

The difference in population dynamics between a system with no behavioral optimization and full rationality Figure 8(1,3) is stark, where the system with

13

bounded rationality has approximately the same dynamics as the one . The resources reach a stable level quickly in all three cases, but the populations of consumers and predators differ markedly. The difference in populations between the system with bounded rationality Figure 8(2) and the fully rational system appears to be negligible, Figure 8(1). The main driver of the change in population dynamics seems to be the ability to retreat to a refuge, and not the exact shape of the distributions when interacting.

4 Discussion

1. Bounded rationality vs full vs empirics

   When looking at ecosystems, there are two main approaches to incorporating behavior:

   (a) Assume perfect rationality

   (b) Ignore it

   The middle way, where animals take rational choices but with a bound on their rationality is typically not included. Imperfect rationality captures that animals might not be perfectly aware of the state of a system, or when distinguishing between almost-equivalent options, choosing the best might require a disprortionate effort. The distribution of copepods in the water column with bounded rationality closely resembles empirical distributions, [?], as the model with perfect rationality suffers from an unphysical discontinuity, also seen in [?]. Comparing the distributions with perfectly rational behavior to the ones with bounded behavior also

2. Population dynamics, short term In short-term models, constant populations are typically assumed [? ? ?]. Though the populations change dramatically over the long term,??, the population levels are essentially unchanged on a daily basis,??. The proposed population-dynamical passes an essential reality test, as wildly fluctuating populations in the short term cannot represent the underlying physical reality. It becomes clear that the near-constant short-term population emerges from the behavorial optimization in the model when comparing to the model with no behavior, ??.

3. Population dynamics, long term When looking at the population dynamics of a predator-prey system through half a year, the seasonal impacts stand out. Even though our model is simple in nature, it can catch essential features as the spring-bloom, and varying phytoplankton throughout the seaonss.

   The long-term patterns are invisible when investigating the short-term fluctuations. As we can see the primary trophic interactions happens in a very short time, the system is fundamentally a slow system driven by a fast underlying dynamic.

4. Distributions throughout the day, snapshot comparison with uffe and toby and Jerome

The migration patterns that we find with our model agree with recent models of vertical migrations, also based on a game-theoretical perspective. This strengthens the conclusions of all three model families, as they are based on fundamentally different numerical and algorithmic schemes.

5. Full migration pattern throughout the day, seasonal differences and empriical findings

   The driver of seasonal variations in migration patterns, is a strong point of the model. Clear variatinos in the expected distributions stand out, and these can theoretically be tested via. echo-acoustics.

6. Model advantages The fitness proxy we use guarantees an ESS, [KC09]. Combing our modeling approach with these theoretical results, it becomes feasible to model multi-actor multi-environment ecosystems. A weakness of the model is, of course, that it does not incorporate a concept of satiation nor ontogenics.

7. Short feeding bouts driving populatino dynamics,

   As short feeding bouts are the drivers of the population dynamics, it becomes quite hard to formulate a long-term model of the slow population dynamics without taking into account the fast feeding dynamics, as these are strongly non-linear and feedback-driven

8. Variation in feeding bouts and relation to migration rationality

   The boundedly rational distributions we arrive at with our model for zooplankton and forage fish seem to agree qualitively with observations to a relatively degree. As such, our model provides a tentative answer to how much realism is lost by the usual assumption of complete rationality. The results we portray show that the overall patterns agree between a population with bounded rationality and one which is completely rational. The usual assumption of complete rational seems to be reasonable modelling assumption, but care should be taken. We show that it is possible to include bounded rationality in a systematic fashion, allowing it as a tuning parameter in future models.

9. Mean-field game The game we study is a mean field game (MFG), where the self-interaction is mediated by the other player. Our game has polymorphic-monomorphic equivalency due to the bilinear nature. Mono-Poly is a necessary requirement for models of DVM, since not all copepods/fish behave exactly the same, and we thereby encapsulate minor variations in each fish.

10. Cost of migration The cost of migration is not incorporated in the model, which it could be. Howver, the cost of mirgation could also be introduced through a proxy where there is a constant species-specific penalty-field incentivizing specific depths, eg. disallowing infinetly deep migrations.

11. Further work - More species, Vinogradov ladder/cascading migrations? The model we have developed is ready-made for incorporating more species. A logical next step would be to examine the concept of cascading migrations and Vinogradovs ladder. Our approach essentially only depends on the linearity of the fitness proxy, so it could be imagined that ontogenics

could be incorporated, via. structuring the populations and considering fitness based on the Leslie matrix, enabling a proxy for life-cycle optimization.

References

[ABB+19] Vincent Acary, Olivier Bonnefon, Maurice Brémond, Olivier Huber, Franck Pérignon, and Stephen Sinclair. *An introduction to Siconos*. PhD thesis, INRIA, 2019.

[AGH+19] Joel A E Andersson, Joris Gillis, Greg Horn, James B Rawlings, and Moritz Diehl. CasADi – A software framework for nonlinear optimization and optimal control. *Mathematical Programming Computation*, 11(1):1–36, 2019.

[And19] Ken H Andersen. *Fish Ecology, Evolution, and Exploitation: A New Theoretical Synthesis*. Princeton University Press, 2019.

[BBM14] Kelly J Benoit-Bird and Margaret A McManus. A critical time window for organismal interactions in a pelagic ecosystem. *PLoS One*, 9(5):e97763, 2014.

[HKM91] SJ Hay, Thomas Kiørboe, and A Matthews. Zooplankton biomass and production in the north sea during the autumn circulation experiment, october 1987–march 1988. *Continental Shelf Research*, 11(12):1453–1476, 1991.

[HO10] Marlis Hochbruck and Alexander Ostermann. Exponential integrators. *Acta Numer.*, 19(May):209–286, 2010.

[HV16] Agnethe N Hansen and André W Visser. Carbon export by vertically migrating zooplankton: an optimal behavior model. *Limnology and Oceanography*, 61(2):701–710, 2016.

[Iwa82] Yoh Iwasa. Vertical migration of zooplankton: a game between predator and prey. *The American Naturalist*, 120(2):171–180, 1982.

[KC09] Vlastimil Krivan and Ross Cressman. On evolutionary stability in predator–prey models with fast behavioural dynamics. *Evolutionary Ecology Research*, 11(2):227–251, 2009.

[Kop09] David A Kopriva. *Implementing spectral methods for partial differential equations: Algorithms for scientists and engineers*. Springer Science & Business Media, 2009.

[MZ91] Douglas A Miller and Steven W Zucker. Copositive-plus lemke algorithm solves polymatrix games. *Operations Research Letters*, 10(5):285–290, 1991.

[NTL+03] LA Fredrik Nilsson, Uffe Høgsbro Thygesen, Bo Lundgren, Bo Friis Nielsen, J Rasmus Nielsen, and Jan E Beyer. Vertical migration and dispersion of sprat (sprattus sprattus) and herring (clupea harengus) schools at dusk in the baltic sea. *Aquatic Living Resources*, 16(3):317–324, 2003.

[OHC+17] M Pilar Olivar, P Alexander Hulley, Arturo Castellón, Mikhail Emelianov, Cristina López, Víctor M Tuset, Tabit Contreras, and Balbina Molí. Mesopelagic fishes across the tropical and equatorial atlantic: biogeographical and vertical patterns. *Progress in Oceanography*, 151:116–137, 2017.

[PV19] Jérôme Pinti and André W Visser. Predator-prey games in multiple habitats reveal mixed strategies in diel vertical migration. *The American Naturalist*, 193(3):E000–E000, 2019.

[SSTM05] David W Sims, Emily J Southall, Geraint A Tarling, and Julian D Metcalfe. Habitat-specific normal and reverse diel vertical migration in the plankton-feeding basking shark. *Journal of Animal Ecology*, pages 755–761, 2005.

[Sut13] TT Sutton. Vertical ecology of the pelagic ocean: classical patterns and new perspectives. *Journal of fish biology*, 83(6):1508–1527, 2013.

[TP18] Uffe H. Thygesen and Toby A. Patterson. Oceanic diel vertical migrations arising from a predator-prey game. *Theoretical Ecology*, 12(1):17–29, 2018.

[VSSK01] AW Visser, H Saito, E Saiz, and Thomas Kiørboe. Observations of copepod feeding and vertical distribution under natural turbulent conditions in the north sea. *Marine Biology*, 138(5):1011–1019, 2001.

[WB06] Andreas Wächter and Lorenz T Biegler. On the implementation of an interior-point filter line-search algorithm for large-scale nonlinear programming. *Mathematical programming*, 106(1):25–57, 2006.

[WDI+14] Zhankun Wang, Steven F DiMarco, Stephanie Ingle, Leila Belabbassi, and Lubna H Al-Kharusi. Seasonal and annual variability of vertically migrating scattering layers in the northern arabian sea. *Deep Sea Research Part I: Oceanographic Research Papers*, 90:152–165, 2014.